

# A COMPREHENSIVE EXPERIMENTAL STUDY ON THE FRICTION STIR WELDING PROCESS FOR JOINING AA6063 ALUMINIUM ALLOY

Regala Aneela<sup>a</sup>, Ajay D Diwate<sup>b</sup>, Ummar Pasha Shaik<sup>c</sup>, Shridhar Rajan Bhasale<sup>d</sup>, Pramod Purandare<sup>e</sup>, Vikas Bhimrao Pawar<sup>f</sup>, Chandrashekhar Ramtirkhar<sup>g</sup>, Rahul Shivaji Yadav<sup>e\*</sup>

**Article history**  
Received  
29 March 2025  
Received in revised form  
20 June 2025  
Accepted  
22 July 2025  
Published online  
28 February 2026

<sup>a</sup>Department of Physics, B V Raju Institute of Technology, Narsapur, Medak, Telangana, 502313, India

<sup>b</sup>Department of Mechanical Engineering, TSSM's Bhivarabai Sawant College of Engineering and Research Narhe, Pune, Maharashtra, 411041, India.

<sup>c</sup>Department of Physics, Anurag Engineering College, Ananthagiri, Suryapet, Telangana, 508206, India

<sup>d</sup>Endurance Technologies Limited, Waluj, Chhatrapati Sambhajnagar, Maharashtra 431136, India

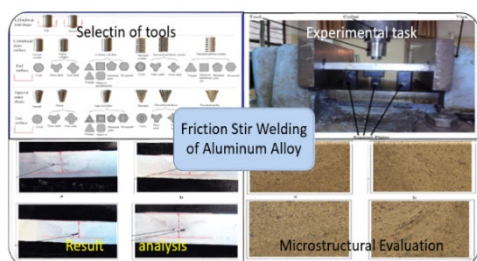
<sup>e</sup>Department of Mechanical Engineering, Marathwada Mitramandal's College of Engineering, Karvenagar, Maharashtra, 411052, India

<sup>f</sup>Department of Applied Science, Bharati Vidyapeeth College of Engineering Navi Mumbai, 400614, India

<sup>g</sup>Department of Mechanical Engineering, Vishwakarma Institute of Information Technology, Kondhwa Budruk, Maharashtra 411048, India

\*Corresponding author  
rahulyadav@mmcoe.edu.in

## Graphical abstract



## Abstract

Despite the widespread use of welding in manufacturing and structural applications, inconsistencies in weld quality remain a significant challenge. Factors such as material flow and heat distribution during the welding process play a critical role in determining the integrity of the weld. This study focuses on using Friction Stir Welding (FSW) to join AA6063 aluminum alloy using a milling machine with a vertical spindle attachment. Four different trials, labeled T1, T2, T3, and T4, are conducted, each with varying welding speeds and tool rotational speeds to explore the impact of these parameters on the weld quality. The tools used in these trials have different threading: M12×1.75 and M8×1, and each has a distinct shoulder diameter. This variation in tool design affects the surface area in contact with the workpiece during welding, which in turn influences heat generation and material flow. The primary goal of these experiments is to assess the weld quality based on several key factors, such as the presence of fractures, porosity, and blow holes, as well as the effect of heat on the grain structure in the welded material, particularly in the heat-affected zone (HAZ). The study demonstrates the milling machine's capability for performing FSW on aluminum alloys, an important aspect for industrial applications where precision and integrity are crucial. The welded joints undergo tensile testing according to ASTM E407-2007 standards. The results show a maximum weld penetration of 8.71 mm, with no cracks or blow holes observed in the joints, indicating high-quality welds. Additionally, the heat-affected zone is visible, reflecting the thermal effects on the material due to the welding process. Overall, the study provides valuable insights into optimizing FSW parameters and highlights the effectiveness of using a milling machine for aluminum alloy welding.

*Keywords:* AA6063, Friction Stir Welding, Microstructure, Welding Plates, Universal Testing Machine.

© 2026 Penerbit UTM Press. All rights reserved

## 1.0 INTRODUCTION

The joining of aluminum alloys, particularly AA6063, is a critical process in various industries such as aerospace, automotive, and

construction, where strong, lightweight materials are required. Traditional welding techniques often struggle with challenges such as distortion, porosity, and the formation of cracks, especially when welding heat-sensitive materials like aluminum. As a result, there is an increasing interest in advanced welding

methods that can offer superior joint quality while minimizing defects. One such promising technique is Friction Stir Welding (FSW), a solid-state welding process known for its ability to join aluminum alloys with minimal thermal distortion and improved mechanical properties. AA6063, an alloy commonly used in structural applications, is particularly suitable for FSW due to its favorable properties, including good corrosion resistance and formability. However, achieving high-quality welds with minimal defects requires careful optimization of welding parameters such as tool rotational speed, welding speed, and tool design. This study investigates the effects of these parameters on the FSW process for joining AA6063 aluminum alloy using a milling machine equipped with a vertical spindle attachment. By varying parameters like tool threading (M12×1.75 and M8×1) and shoulder diameter, this research aims to understand their impact on weld quality, specifically regarding material flow, heat distribution, and the resultant weld integrity.

## 2.0 LITERATURE REVIEW

Friction Stir Welding (FSW) is a solid-state joining process that has revolutionized the welding of lightweight materials, particularly aluminium alloys. AA6063, a heat-treatable aluminium alloy, is widely used in structural applications due to its excellent extrudability, corrosion resistance, and moderate strength.

### 2.1 Process Parameters of FSW

The quality of FSW joints is highly influenced by process parameters such as tool rotational speed, welding speed, axial force, and tool geometry. These parameters determine the heat generation, material flow, and the weld integrity.

**Tool Rotational Speed:** Studies by Mishra and Ma [1] and Elangovan and Balasubramanian [2] highlight that rotational speed significantly affects heat input and material mixing. For AA6063, an optimal range of 800–1200 rpm is recommended to achieve defect-free welds with improved mechanical properties. Higher speeds may cause excessive flash, while lower speeds can lead to insufficient heat input.

**Welding Speed:** Research by Threadgill et al. [3] and Zhang et al. [4,5] demonstrates that welding speed influences the cooling rate and heat distribution. Lower welding speeds (50–100 mm/min) are preferred for AA6063 to ensure adequate material flow and avoid defects like tunnel voids.

**Axial Force:** The axial force ensures proper consolidation of the weld material. Studies by Kumar and Kailas [6] and Rajakumar et al. [7] indicate that an optimal axial force of 2–6 kN is critical for achieving sound welds in AA6063. Insufficient force can cause voids, while excessive force may lead to tool wear and surface defects.

**Tool Geometry:** The design of the tool pin and shoulder plays a crucial role in material flow and heat generation. Research by Buffa et al. [8] and Genevois et al. [9] shows that tools with threaded pins and concave shoulders enhance material mixing and produce superior weld quality in AA6063.

### 2.2 Mechanical Properties

The mechanical properties of FSW joints, including tensile strength, hardness, and fatigue resistance, are critical for industrial applications. Numerous studies have evaluated these properties for AA6063 aluminum alloy.

Studies by Cavaliere et al. [10] and Su et al. [11] demonstrate that Friction Stir Welding (FSW) joints of AA6063 aluminum alloy achieved 85–95% of the base metal's tensile strength. This high strength is attributed to the fine-grained microstructure formed in the stir zone (SZ) due to dynamic recrystallization during the welding process. The refined grains enhance mechanical properties, making FSW a reliable method for joining AA6063 with minimal loss in tensile strength compared to traditional welding techniques.

The hardness distribution across the weld zone is primarily dictated by microstructural transformations that occur due to thermal and mechanical effects. Rhodes et al. [12-13] and Fonda et al. [14] observed that the stir zone (SZ) exhibits increased hardness, attributed to significant grain refinement caused by dynamic recrystallization during welding. In contrast, the heat-affected zone (HAZ) experiences a reduction in hardness due to thermal softening, which results from the coarsening of grains and the dissolution of strengthening precipitates. These variations in hardness influence the overall mechanical properties of the welded joint, impacting its strength, toughness, and resistance to failure under load.

Friction stir welded (FSW) joints of AA6063 demonstrate superior fatigue resistance compared to fusion-welded joints. Research by Lomolino et al. [15] and Zhang et al. [16-17] attributes this advantage to the weld zone's defect-free nature and uniform microstructure. Unlike fusion welding, which often introduces porosity, cracks, and metallurgical inconsistencies, FSW promotes grain refinement and eliminates solidification defects. The enhanced microstructural integrity reduces stress concentrations and improves load-bearing capacity under cyclic loading. As a result, FSW joints exhibit prolonged fatigue life, making them highly suitable for structural applications requiring durability and resistance to fatigue-induced failure.

The conventional arc welding, friction stir welding and rotary friction welding are also very popular and a lot of work has been reported on materials joined by these processes [18]. The ability to join huge and small size parts, in a variety of similar and dissimilar materials, shapes and sizes make LFW unparalleled. Such joint configurations are very common in transportation sectors including aerospace and railways [19].

The effectiveness of Friction Stir Welding (FSW) in AA6063 aluminum alloy largely depends on the design and material of the welding tool. Key factors include tool geometry and material selection, both of which impact process parameters. The FSW tools as shown in figure 1 and figure 2 consists of a shoulder and a pin, where the shoulder diameter influences heat generation and pressure distribution. Pin geometry, such as flat or domed ends, affects deformation, heating, and applied forces. Triangular or trifled pins improve material flow over cylindrical designs, while threaded pins enhance heat input. Selecting a wear-resistant tool material is essential. Various pin shapes optimize material mixing and weld quality.

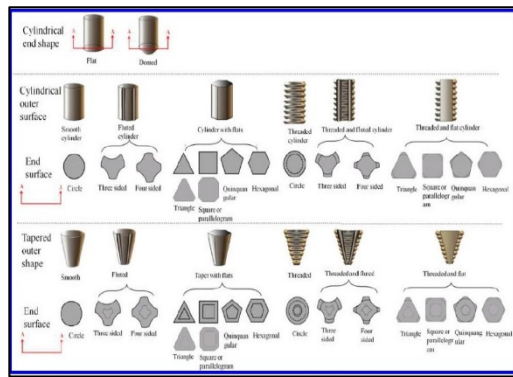


Figure 1 FSW Tool Probes [18]



Figure 2 FSW tool of threading M8x1 (Tool I)



Figure 3 FSW tool of threading M12x1.75 (Tool II)

Table 1 parameters and different tools used for experimental trails

Parameter	Description	
	Tool I	Tool II
Shoulder Diameter (mm)	27	20
Tool Pin Profile	Cylindrical Threaded Pin	Cylindrical Threaded Pin
Threading	M8x1	M12x1.75
Pin Diameter (major) (mm)	7.90	11.90
Ecimen	6.70	9.95
Pin Diameter (minor) (mm)		
Pin Length (mm)	7.3	7.4
Tool Shank (Diameter)(mm)	20	20
Shoulder Length	30	30

### 2.3 Microstructure Evaluation

The microstructural characteristics of friction stir welded (FSW) joints play a crucial role in defining their mechanical properties. Research on AA6063 primarily focuses on three aspects: grain refinement, precipitate distribution, and texture evolution, each contributing to the overall performance of the weld.

Dynamic recrystallization during FSW significantly refines grains in the stir zone (SZ). Studies by Mishra and Ma [1] and Genevois et al. [21] report that grain sizes in the SZ of AA6063 can be reduced to 2–5 μm, a substantial improvement compared to the base metal. This grain refinement enhances both strength and toughness by limiting dislocation movement and improving resistance to crack initiation. The thermal cycle in FSW affects the distribution and stability of strengthening precipitates in AA6063, particularly Mg<sub>2</sub>Si precipitates. Research by Su et al. and Fonda et al. [22] shows that in the heat-affected zone (HAZ), the precipitates undergo coarsening, leading to a drop in hardness due to the dissolution and precipitation of strengthening phases. Conversely, the SZ retains a finer dispersion of precipitates, contributing to improved hardness and strength compared to the HAZ. Severe plastic deformation during FSW leads to the formation of distinct crystallographic textures. Studies by Threadgill et al. [3] and Zhang et al. [23-25] reveal that the SZ of AA6063 develops a shear texture, which directly influences the anisotropy of mechanical properties. This shear texture affects the direction-dependent behavior of strength and ductility, making it essential to consider during structural applications. Overall, the combined effects of grain refinement, precipitate distribution, and texture evolution define the superior mechanical performance of AA6063 FSW joints compared to traditional fusion welding methods.

### 2.4 Specimen Preparation and Experimental Setup

The experimental procedure primarily consists of two key stages: specimen preparation and the actual experimentation. In the specimen preparation phase, raw material in the form of long strips of AA6063 aluminum alloy was procured and cut into samples of desired dimensions as shown in Table 2. These samples were then further machined using a milling machine equipped with a surface cutter to ensure uniformity in dimensions and flatness. Special attention was given to achieving precise alignment, ensuring that the plates fit perpendicularly within the jaws of the vise without any deviation along their length. This step was critical to maintaining consistency and accuracy during the welding trials. The flattening process, carried out using the surface cutter, is illustrated in Figure 4, which provides a visual representation of the setup and methodology employed. This meticulous preparation ensured that the specimens were ready for subsequent friction stir welding trials under controlled and repeatable conditions as shown in Figure 5.

The experiment involves mounting the test Plates as shown in figure 6 in a vise with support plates beneath them to prevent movement and minimize vibrations. The support plate also aids in heat dissipation, As shown in figure 7 different temperature sensors are used to measure temperature/heat at different locations transferring frictional heat to the base while maintaining low thermal conductivity to enhance joint strength. Steel support plates were used due to their minimal thermal conductivity and ability to restrict lateral movement. The tools,

shown in Figure 3, and specifications are mentioned in Table 1 were mounted in a 20mm collet and secured using a torque wrench. Four trials as mentioned in Table 3 were conducted, using each tool twice for four weld specimens, with parameters selected based on machine specifications and literature review.



Figure 4 Surfacing of the specimen

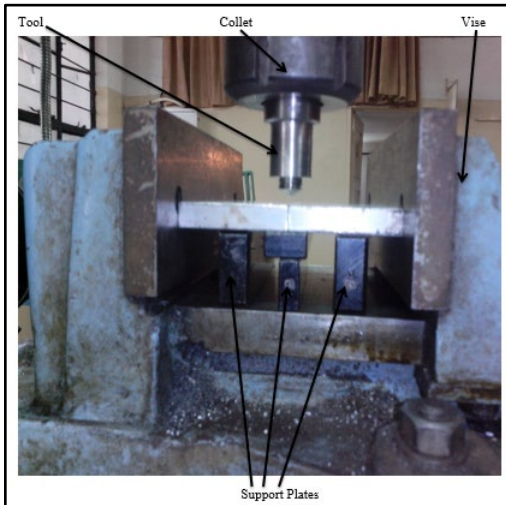


Figure 5 Actual Experimental Set up of AA6063

Table 3 Process Parameters for FSW of AA6063 [24]

Parameter	Friction Stir Welding Trials			
	T1	T2	T3	T4
<b>Tool Type</b>	Cylindrical Threaded	Cylindrical Threaded	Cylindrical Threaded	Cylindrical Threaded
<b>Threading of the tool</b>	M12×1.75	M12×1.75	M8×1	M8×1
<b>Shoulder Diameter (mm)</b>	20	20	27	27
<b>Shoulder length (mm)</b>	30	30	30	30
<b>Tool Pin Length(mm)</b>	7.4	7.4	7.3	7.3
<b>Tool Rotating Speed (rpm)</b>	720	720	510	510
<b>Welding Speed (mm/min)</b>	0.869	1.65	2.70	8.645

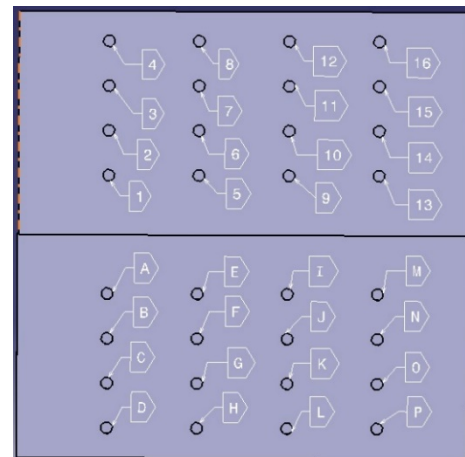


Figure 6 Array of holes with nomenclature

Table 2 Plate Dimensions after Surfacing

Plates in Joint	Friction Stir Welding Trials			
	T1	T2	T3	T4
<b>Plate 1</b>	51×150	51×150	80×150	80×150
<b>Plate 2</b>	51×150	51×150	80×150	80×150

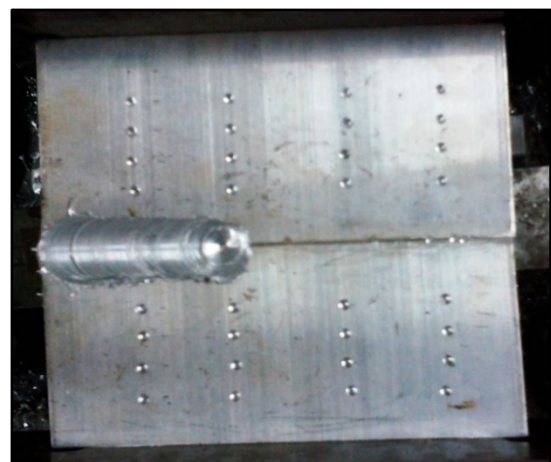


Figure 7 Actual Workpiece for temperature measurement

### 3.0 RESULTS AND DISCUSSION

The tensile test of the welding joint samples was conducted on UTM and the test results are as mentioned in Table 4. The testing results of the welded joints, conducted by the “ASTM E407-2007” standards, are illustrated in Figures 8. These results provide a detailed analysis of weld penetration, structural integrity, and microstructural characteristics of the welded joints across four trials (T1 to T4). In trial T1, the weld penetration measured 8.71 mm, which was the highest among the four trials. No cracks or blowholes were observed in the welded joint, indicating good structural integrity. However, a heat-affected zone (HAZ) was identified in the welded joint region, which was typical in welding processes due to thermal cycling. The microstructure of the weld area exhibited elongated grains, a common feature in welded joints resulting from the directional solidification of the molten metal. Trial T2 showed a weld penetration of 8.56 mm, slightly lower than T1.

**Table 4** Tensile Test Results

Parameters	Samples			
	T1	T2	T3	T4
Tensile Strength (KN)	32	31	27	25

However, a crack was observed under microscopic examination, suggesting potential stress concentration or improper cooling. Like T1, a HAZ was present, and the microstructure displayed elongated grains. In trial T3, the weld penetration was 7.02 mm, the lowest among the trials. Minor porosity was detected in the weld joint, which could weaken the joint’s mechanical properties. The HAZ and elongated grain structure were also observed. Trial T4 exhibited a weld penetration of 7.98 mm, with a single crack and slight porosity in the weld region. The presence of cracks and porosity indicates potential issues with welding parameters or material quality. The HAZ and elongated grains were consistent with the other trials. Overall, the results highlight the variability in weld quality across trials, with T1 being the most optimal due to its high penetration and absence of defects. The consistent presence of HAZ and elongated grains underscores the influence of thermal effects on the microstructure of welded joints.

#### 3.1. Microstructural Analysis

The microstructure evaluation of Aluminum Alloy AA6063 was conducted according to the ASTM E407-2007 standard. The sample was carefully sectioned along its transverse orientation to expose the grain structure as clearly as possible. After polishing the surface to a mirror-like finish, hydrofluoric acid was used as the etchant—a method chosen for its ability to effectively reveal the fine details of aluminum microstructures. The etching process was handled with care to avoid over-etching, ensuring the grain boundaries stood out without any distortion. When the sample was examined under the microscope, elongated grains came into clear view, showcasing the material’s typical response to processing. The typical results for all the four samples are tabulated in the Table 1

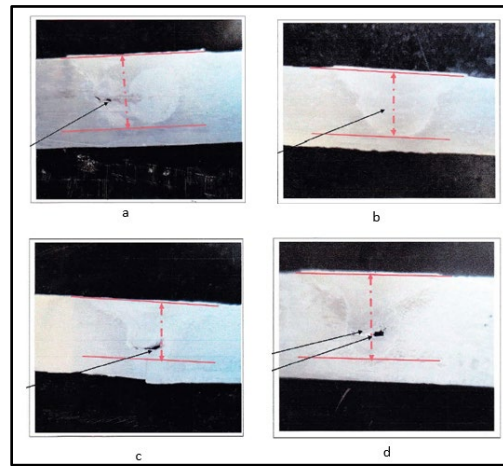


**Figure 8** Testing results of all four samples T1, T2, T3, and T4 r

**Table 5** Testing results after evaluation for all four samples

Parameters	Samples			
	T1	T2	T3	T4
Total Weld Depth (mm)	8.71	8.56	7.02	7.98
Crack	Not observed	Observed	Not observed	Observed
Blow Holes	Not observed	Not observed	Not observed	Not observed
Heat Affected Zone	Observed	Observed	Observed	Observed
Effect on grain structure	Elongated grains observed	Elongated grains observed	Elongated grains observed	Elongated grains observed
Tensile Strength (KN)	32	31	27	25

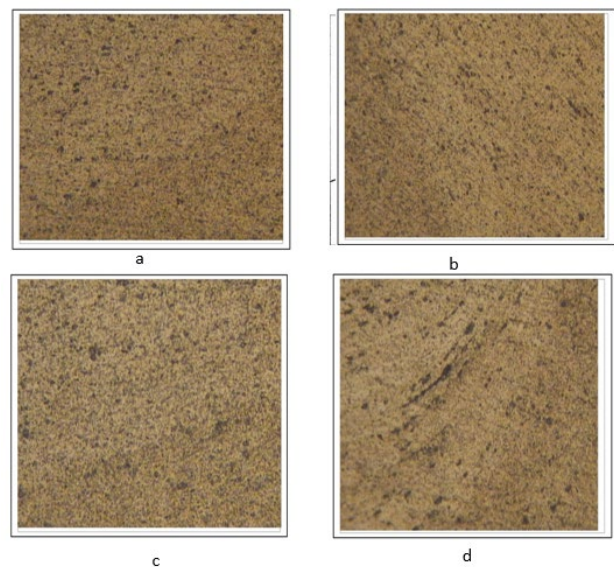


**Figure 9** Microstructural evaluation of all four samples T1, T2, T3, and T4 respectively

The analysis of weld penetration and microstructural characteristics as shown in Figure 9 across different trials provides critical insights into the quality and integrity of laser-welded joints. In Trial T1, the weld exhibited a penetration depth of 8.71 mm, with no visible cracks or blowholes, indicating optimal welding conditions. The presence of a heat-affected zone (HAZ) was noted, which was expected due to localized thermal effects. This suggests that the process parameters used in T1 effectively balanced heat input and penetration, minimizing defect formation. In contrast, Trial T2 demonstrated a slightly lower penetration depth of 8.56 mm, but microscopic analysis revealed the presence of a crack. This indicates that even when similar weld penetration is achieved, underlying issues like internal stress or thermal gradients can still lead to crack formation. These cracks are likely the result of uneven cooling rates or differences in material properties at the fusion boundary—subtle factors that often go unnoticed but can significantly impact the weld's durability and long-term performance. Understanding these nuances is crucial to preventing failures and ensuring the reliability of welded structures. Trial T3 exhibited the lowest penetration depth at 7.02 mm, with minor porosity observed in the weld joint. All the testing observations are tabulated in Table 5. The presence of porosity indicates potential issues related to gas entrapment or improper shielding during the welding process, which can weaken mechanical properties. Similarly, Trial T4 resulted in 7.98 mm of weld penetration, accompanied by a single crack and minor porosity. The appearance of both defects suggests suboptimal process parameters, possibly involving excessive heat input or insufficient filler material distribution. Across all trials, the presence of a heat-affected zone and elongated grains in the weld microstructure confirms significant thermal influence during welding. These findings emphasize the need for precise parameter optimization to achieve defect-free welds with consistent penetration and structural integrity.

### 3.2 Failure Mode Study and Ultimate Failure Load

Following the experimentation and analysis of Friction Stir Welding (FSW) and the subsequent testing of welded joints, several critical findings had been identified, which provided valuable insights into the optimization of the FSW process. These findings were discussed below in the context of their implications for weld quality and process parameters.

### 3.3 Tool Dimensions and Plate Length

Based on the experimental findings, it was observed that the shoulder diameter of the welding tool plays a significant role in determining the ultimate tensile strength (UTS) of the welded joint. When the shoulder diameter was maintained at 20 mm, the resulting joint exhibited the highest tensile strength, ranging between 31–32 kN. This indicates that at this specific diameter, the tool was able to generate optimal heat input and material flow, leading to a strong and well-bonded weld. However, as the shoulder diameter was increased beyond 20 mm, a noticeable decline in tensile strength was recorded, with values dropping to between 25–27 kN. This reduction suggests that a larger shoulder diameter may introduce excessive heat into the weld zone, potentially causing overheating, grain coarsening, or undesirable thermal gradients. These factors can negatively

affect the microstructure of the weld, leading to weaker joints. The results highlight the importance of optimizing tool geometry, particularly shoulder diameter, to achieve the best possible weld quality. A careful balance must be struck, as too small a diameter may not generate sufficient heat, while too large a diameter can compromise the structural integrity of the joint.

### 3.4 Tool Speed and Temperature Generation

The rotational speed of the tool was a key parameter that must be optimized based on the plate thickness and tool diameter. Higher tool speeds were generally advantageous as they generate elevated temperatures, which were essential for effective material plasticization and flow [26-27]. The weld quality was directly proportional to the temperature achieved during the process, with higher temperatures resulting in improved weld aesthetics and mechanical properties. The weld speed was at 720 rpm the strength was quite higher than that of the 510 rpm speed. The ultimate tensile strength of the joint is decreased from 31Mpa to 25 Mpa. This highlights the importance of selecting an appropriate tool speed to achieve optimal thermal conditions.

### 3.5 Tool Pin Length and Plunge Depth

The length of the tool pin significantly affects the plunge depth and the extent of material mixing during FSW. A longer pin length allows for deeper penetration into the workpiece, facilitating a larger swirling action and better material intermixing [28]. This results in stronger and more homogeneous welds. The tool pin length was changed from 7.4 mm to 7.3 mm a significant change is observed in the tensile strength, and was reduced from 32 KN to 25 KN. However, the pin length must be carefully controlled to ensure it did not exceed the plate thickness, as excessive penetration could lead to tool wear or improper weld formation.

### 3.6 Clamping and Heat Dissipation

The clamping and support arrangements used during FSW act as heat sinks, dissipating heat from the weld zone. While this could prevent overheating and distortion, it may also lead to localized hardening and reduced tensile strength in the clamped regions due to rapid cooling [29]. This underscores the need for balanced heat management during the welding process to minimize adverse effects on the mechanical properties of the weld.

### 3.7 Material Flow and Cracks

The design of the tool pin, particularly its threaded structure, plays a crucial role in determining the quality of the weld. Tools with complex geometries, such as trivex or trifluted pins, or those featuring multiple flat surfaces, exhibit superior material mixing capabilities compared to conventional cylindrical threaded tools [30]. As the temperature increases along with tool speed increases the cracks are observed in the microstructures. The depth of heat affected zones are observed with elongated grain structures which are directly affected on tensile strength of the joints. These advanced geometries enhance material flow and intermixing, resulting in stronger and more uniform welds.

## 4.0 CONCLUSION

The experimental analysis of welded joints, conducted by ASTM E407-2007 standards, revealed variations in weld penetration, defect formation, and microstructural characteristics. Trial T1 which is having maximum tool pin length with 720 rpm with minimum welding speed 0.869 mm/min exhibited the highest weld penetration (8.71 mm) without cracks or blowholes. In contrast, trials T2, T3, and T4 showed decreasing penetration values with the presence of defects such as cracks and porosity. The heat-affected zone and elongated grains in the welding area's microstructure were consistently observed across all trials. These findings highlight the influence of welding conditions on joint integrity and suggest the need for further optimization to enhance weld quality and minimize defects.

### Acknowledgment

We would like to acknowledge Marathwada Mitra Madal's College of Engineering for providing access to their laboratory facilities for conducting the flexure test in this study.

### Conflicts of Interest

The author(s) declare(s) that there is no conflict of interest regarding the publication of this paper

### References

- [1] Mishra, R. S., & Ma, Z. Y. 2005. Friction stir welding and processing. *Materials Science and Engineering: R: Reports*, 50(1-2): 1-78.
- [2] Elangovan, K., & Balasubramanian, V. 2008. Influences of tool pin profile and welding speed on the formation of friction stir processing zone in AA6063 aluminium alloy. *Journal of Materials Processing Technology*, 200(1-3): 163-175.
- [3] Threadgill, P. L., Leonard, A. J., Shercliff, H. R., & Withers, P. J. 2009. Friction stir welding of aluminium alloys. *International Materials Reviews*, 54(2): 49-93.
- [4] Zhang, Z., Zhang, H. W., & Xu, L. 2020. Machine learning-based optimization of friction stir welding parameters for AA6063 aluminium alloy. *Journal of Manufacturing Processes*, 56: 1-10
- [5] Zhang, Z., & Chen, D. L. 2008. Consideration of Orowan strengthening effect in particulate-reinforced metal matrix nanocomposites: A model for predicting their yield strength. *Scripta Materialia*, 58(11): 1027-1030.
- [6] Kumar, K., & Kailas, S. V. 2008. The role of friction stir welding tool on material flow and weld formation. *Materials Science and Engineering: A*, 485(1-2): 367-374.
- [7] Rajakumar, S., Muralidharan, C., & Balasubramanian, V. 2011. Influence of friction stir welding process and tool parameters on strength properties of AA6063-T6 aluminium alloy joints. *Materials & Design*, 32(2): 535-549.
- [8] Buffa, G., Hua, J., Shivpuri, R., & Fratini, L. 2006. Design of the friction stir welding tool using the continuum based FEM model. *Materials Science and Engineering: A*, 419(1-2): 381-388.
- [9] Genevois, C., Deschamps, A., Denquin, A., & Doisneau-Cottignies, B. 2005. Quantitative investigation of precipitation and mechanical behaviour for AA2024 friction stir welds. *Acta Materialia*, 53(8): 2447-2458
- [10] Cavaliere, P., Nobile, R., Panella, F. W., & Squillace, A. 2006. Mechanical and microstructural behaviour of 2024–7075 aluminium alloy sheets joined by friction stir welding. *International Journal of Machine Tools and Manufacture*, 46(6): 588-594.
- [11] Su, J. Q., Nelson, T. W., Mishra, R., & Mahoney, M. 2003. Microstructural investigation of friction stir welded 7050-T651 aluminium. *Acta Materialia*, 51(3): 713-729.
- [12] Rhodes, C. G., Mahoney, M. W., Bingel, W. H., & Calabrese, M. 1997. Fine-grain evolution in friction-stir processed 7050 aluminium. *Scripta Materialia*, 36(1): 69-75.
- [13] Rhodes, C. G., & Mahoney, M. W. 1996. Fine-grain evolution in friction-stir processed 7050 aluminium. *Scripta Materialia*, 36(1): 69-75.
- [14] Fonda, R. W., Bingert, J. F., & Colligan, K. J. 2004. Development of grain structure during friction stir welding. *Scripta Materialia*, 51(3): 243-248.
- [15] Lomolino, S., Tovo, R., & dos Santos, J. 2005. On the fatigue behaviour and design curves of friction stir butt-welded Al alloys. *International Journal of Fatigue*, 27(3): 305-316.
- [16] Zhang, Z., Zhang, H. W., & Xu, L. 2020. Machine learning-based optimization of friction stir welding parameters for AA6063 aluminium alloy. *Journal of Manufacturing Processes*, 56: 1-10.
- [17] Zhang, Z., & Chen, D. L. 2008. Consideration of Orowan strengthening effect in particulate-reinforced metal matrix nanocomposites: A model for predicting their yield strength. *Scripta Materialia*, 58(11): 1027-1030.
- [18] Gangil N, Mishra A, Lone NF, Bajaj D, Chen D, Haider J, Chen X, Kononov S, Siddiquee AN. 2025. Linear Friction Welding of Similar and Dissimilar Materials: A Review. *Metals and Materials International*. 31(1): 1-21.
- [19] Mojtaba Farbakhti, Seyed Reza Elmi Hosseini, Seyed Ali Mousavi Mohammadi, Sadaf Sadatabhari, Huo Yuan-ming, Ruifeng Li, 2025, Similar and dissimilar rotary friction welding of steels: A review of microstructural evolution and mechanical properties, *Journal of Materials Research and Technology*, 36: 8777-8803, DOI: <https://doi.org/10.1016/j.jmrt.2025.05.079>.
- [20] Y. N. Zhang, X. Cao, S. Larose and P. Wanjara, 2012. Review of tools for friction stir welding and processing, National Research Council Canada, *Canadian Metallurgical Quarterly*, 51(3): 250-259.
- [21] Genevois, C., Deschamps, A., Denquin, A., & Doisneau-Cottignies, B. 2005. Quantitative investigation of precipitation and mechanical behaviour for AA2024 friction stir welds. *Acta Materialia*, 53(8): 2447-2458.
- [22] Fonda, R. W., & Bingert, J. F. 2004. Microstructural evolution in the heat-affected zone of a friction stir weld. *Metallurgical and Materials Transactions A*, 35(5): 1487-1499.
- [23] Zhang, H., Wang, X., & Wang, G. 2013. Optimization of friction stir welding parameters for AA6063 aluminium alloy using response surface methodology. *Journal of Materials Engineering and Performance*, 22(10): 2934-2941
- [24] Zhang, Z., & Chen, D. L. 2008. Consideration of Orowan strengthening effect in particulate-reinforced metal matrix nanocomposites: A model for predicting their yield strength. *Scripta Materialia*, 58(11): 1027-1030.
- [25] Zhang, H., Wang, X., & Wang, G. 2014. Optimization of friction stir welding parameters for AA6063 aluminium alloy using artificial neural network. *Journal of Materials Engineering and Performance*, 23(12): 4341-4348.
- [26] S. R. Bhasale, M. S. Wadekar 2015, Friction Stir Welding of AA6063- Experimentation and Testing, *International Journal of Innovations in Engineering, Research and Technology*, 2(7): 1- 11
- [27] Thomas, W. M., Nicholas, E. D., Needham, J. C., Murch, M. G., Temple-Smith, P., & Dawes, C. J. 1991. Friction stir butt welding. *International Patent Application* No. PCT/GB92/02203.
- [28] Scialpi, A., De Filippis, L. A. C., Cavaliere, P., & Squillace, A. 2007 Influence of shoulder geometry on microstructure and mechanical properties of friction stir welded 6082 aluminium alloy. *Materials & Design*, 28(4): 1124-1129.
- [29] Sutton, M. A., Reynolds, A. P., Yang, B., & Yuan, N. 2002. Microstructure and mixed-mode I/II fracture of AA2524-T351 base material and friction stir welds. *Engineering Fracture Mechanics*, 69(14-16): 1605-1623.
- [30] Threadgill, P. L., Leonard, A. J., Shercliff, H. R., & Withers, P. J. 2009. Friction stir welding of aluminium alloys. *International Materials Reviews*, 54(2): 49-93.